Numerical and experimental studies on laminar hydrodynamic and thermal characteristics in fractal-like microchannel networks. Part A: Comparisons of two numerical analysis methods on friction factor and Nusselt number

Chun-ping Zhang [a,b], Yi-fu Lian [b], Xiang-fei Yu [a], Wei Liu [a,c], Jyh-tong Teng [b,*], Ting-ting Xu [a], Cheng-Hsing Hsu [b], Yaw-Jen Chang [b], Ralph Greif [d]

[a] School of Energy and Power Engineering, Huazhong University of Science and Technology, Wuhan 430074, PR China
[b] Department of Mechanical Engineering, Chung Yuan Christian University, Chungli 32023, Taiwan
[c] Wuhan University of Technology, Wuhan 430074, PR China
[d] Department of Mechanical Engineering, University of California at Berkeley, CA 94720, USA

ARTICLE INFO	ABSTRACT
	In this paper, the conventional equivalent method and the subsectional integral method were used to analyze the friction factor and the Nusselt number in fractal-like microchannel networks. The calculated results obtained from the two methods were compared with those obtained from the experimental data. It was proved that for complex configuration of the microchannel, the conventional equivalent method based on the parameters of inlet and outlet has larger deviations than the subsectional integral method developed in the present study. Furthermore, the results from the subsectional integral method were verified to agree well with those from the experiments under different boundary conditions. In addition, the effects of both hydrodynamically and thermally developing flow were taken into considerations since the bifurcations and bends in the fractal-like microchannel networks disturbed the flow and made the developing flow maintain in each branch. And these effects have been included by replacing the Fanning friction factor with the apparent friction factor to account for the frictional and developing flow pressure drops.

1. Introduction

As the famous Moore's law had predicted, the power and integrated level of the electronic devices, e.g. micro-processor, have increased rapidly in the past few decades. In the irresistible trend of high heat flux density, the failure rates of the microelectronic devices as a result of overheating have increased greatly. Thus, the effective and feasible methods of the thermal management are urgently needed. Since the pioneering work done by Tuckerman and Pease [1], the microchannel heat sinks have been introduced as an attractive and potential option for electronics cooling, drawing substantial interests in the study of the flow and heat transfer characteristics in the microchannels [2–7].

For practical applications, the single microchannel cannot satisfy the requirement associated with the large cooling power. Although the parallel microchannels can offer relatively large heat transfer area using optimization methodology, there are two

serious weaknesses which are difficult to overcome [8–11]. One is the high pressure difference between the two ends of the channels which leads to a high pressure loss. The other is the nonuniform wall temperature distribution due to the fluid temperature increase along the channel. The temperature distribution has a direct impact on the performance in many important applications, e.g. the chips and the fuel cells cooling; the thermal management is subject to the constraint of a maximum temperature difference within the system. The hot spots need to be avoided, and the provision of a spatially uniform temperature distribution would be desirable.

Inspired by the natural flow systems such as mammalian circulatory and respiratory ones, Bejan and Errea [12,13] introduced the "constructal" or "fractal" microchannel network as heat sinks for the electronic devices. They studied the cooling performance of the rectangular and the disk-shaped hierarchical structured networks, and proposed designs for fluid flow with minimum flow resistance. Recently, Bejan [14,15] used the constructal theory to explain the flow configuration from volume-to-point, such as the animal body heat loss and the hot water distribution on a specified

* Corresponding author. Tel.: +886 3 2654308; fax: +886 3 2654399.
  E-mail address: tengcycu@hotmail.com (J.-t. Teng).

Nomenclature

c_p	specific heat at constant pressure
COP	coefficient of performance
D_h	hydraulic diameter
f	Fanning friction factor
f_{app}	apparent friction factor
f_x	local friction factor
$K(x)$	incremental pressure defect
L	microchannel length
L_h	hydrodynamically developing region
L_t	thermal entry length
Nu	Nusselt number
Nu_x	local Nusselt number
P_o	Poiseuille number
P_r	Prandtl number
ΔP	pressure loss
Re	Reynolds number
T	temperature
u_m	average flow velocity
x^*	characteristic length of Nusselt number

x	length from entrance
x^+	characteristic length of friction factor

Greek symbols

α	aspect ratio
λ	thermal conductivity
μ	dynamic viscosity
ρ	density

Subscripts

fd	fully developed condition
i	inlet
m	arithmetic mean
n	level number
o	outlet
$x,3$	location for the three-sided heating case
$x,4$	location for the four-sided heating case

territory. The theory showed that the fractal-like optimized architecture could effectively minimize the pumping power and enhance the convective heat transfer to achieve high thermo-fluid performance.

Pence [16] and Alharbi et al. [17,18] analyzed a fractal-like bifurcating microchannel network for the convective cooling of microelectronic components with geometric disk shapes. Under the same pumping power, the total flow rate, and the total convective surface area, the fractal-like channel network yielded a 60% lower pressure drop and a 30 K lower wall temperature than the straight array channels. A lower channel packing density of the fractal-like channel network (i.e., the convective surface area is 50% less than that of the straight array channel) yielded approximately the same pressure drop and the maximum wall temperature under the fixed-flow-rate conditions. Then Heymann et al. [19] optimized the fractal-like branching flow networks using one-dimensional model for the minimum pressure drop and the flow power through the methods of a direct numerical search and a genetic algorithm. In particular, Daniels et al. [20,21] extended the application of a tree-like network from a single phase flow to a two-phase flow and investigated the adiabatic flow boiling in such a microchannel network by experiment and simulation.

Senn and Poulikakos [22,23] presented a three-dimensional forced convective model for tree-like microchannel networks with the constant wall heat flux for the thermal management in polymer electrolyte fuel cells. The effects of the secondary flow initiated at the bifurcations on the flow and thermal mixing were investigated numerically. It was found that the tree-like network with six branching levels resulted in almost half the pressure drop than the corresponding serpentine flow pattern under the same conditions of surface area and inlet Reynolds number. Laminar mixing by the secondary flow motions substantially improved the local Nusselt numbers. Much higher heat transfer coefficients were obtained from the tree-like network. Then they introduced this kind of structure as a fuel cell fluid distribution concept to optimize the design of the pyramidal direct methanol fuel cells [24].

Escher et al. [11] used a one-dimensional model to analyze the hydrodynamic and thermal performances of a bifurcating and a parallel channel networks under different boundary conditions. The parallel network had 121 parallel microchannels with a heat

transfer surface of 28 cm^2, while the total surface area of the tree-like network was just 2.1 cm^2, which they demonstrated that a restriction in the surface area was not an appropriate boundary condition for comparison of efficiency with different heat sink designs in realistic electronics applications. The compared results showed that the parallel channel cooler had more than fivefold higher coefficient of performance than the bifurcating tree-like network for a constant flow rate, while almost four times more heat could be removed for a constant pressure gradient across the networks. However, they also indicated that the design drawback of the parallel channels was the nonuniformity in the cooling capability owing to the heating up of the fluid in the axial direction along the channels.

Wang et al. [25–27], using numerical simulations, demonstrated the advantages of the fractal-like microchannel network such as the lower flow resistance, temperature uniformity, and reduction of the blockage danger compared with the traditional serpentine and parallel microchannels. In addition, various optimized designs with parameters such as the branch numbers, branching level numbers, and channel numbers reaching the center of the disk were addressed. At the same time, they also showed that the bifurcation angles and two-dimensional roughness had important effects on the performance of the microchannel cooling [28].

Chen and Cheng [29,30] studied the fractal-like network both in minichannels and microchannels. Firstly, they designed a new sandwich structure fractal-like channel network (with a rectangular cross-section) in order to solve the free circulation problem of the cooling fluid. Then, a comparison with the traditional parallel microchannels showed that the new fractal-like microchannel network had a stronger heat transfer capability and required lower pumping power with a large fractal dimension or a high total number of branching levels. Moreover, the experimental investigation confirmed that the thermal efficiency of the fractal-like microchannel network with the branching levels less than 4 was much higher than that of the traditional parallel microchannels. And the pressure loss of bifurcations could be neglected. Then, Chen and Zhang [31] developed a three-dimensional thermal and hydrodynamic model for a fractal-like minichannel heat sink with the consideration of the conjugate heat transfer in the channels. They found that in fractal-like network, the local pressure loss due to the confluence flow was larger than that due to the diffluence flow. However, both

the simulated and experimental results showed that the fractal-like minichannel heat sink had much lower total pressure drop, uniform temperature distribution, and a COP which was two times of that for the traditional serpentine channel. Lately, Chen and Zhang [32,33] used the fractal-like networks with sandwich structure for the study of two-phase boiling flow and for the design of a methanol steam microreactor. The results obtained from the simulations verified that the performances of the fractal-like network for the conditions under their studies were better than the corresponding serpentine channels under the same working conditions.

Haller and Woias [34] found that the shape of the bends and branches, e.g. L-bends and T-joints had significant influences on the pressure loss and the heat transfer. Their study indicated that the pressure loss and the heat transfer in the bends and joints led to a higher cooling ability and a higher effectiveness for the cooling system. Soupremanien et al. [35] conducted experimental study of the influence of the aspect ratio on the boiling flows in single rectangular minichannels with the same hydraulic diameter. The heat transfer efficiency was high when the channel had the lowest aspect ratio under the low heat flux conditions. But if the heat flux was high, the channel with the highest aspect ratio performed best. Their study showed that the characteristics of the flow and the heat transfer were significantly influenced by the shape of bends, the number of branches, the aspect ratio of channels, and the hydraulic diameter.

Through the above reviews on the state-of-the-art of the fractal-like microchannels' research, it was found that most of the analyses were under the assumptions: (1) laminar and incompressible steady flow, (2) constant fluid and solid properties, and (3) hydrodynamically and thermally fully developed flow. But Senn and Poulikakos [23] and Escher et al. [11] indicated that only for the large length/diameter ratios and the low Reynolds numbers, the thermal and flow developed lengths with respect to the channel length could be neglected; and the assumption of (3) would be adequate. Although some researchers [36–38] have considered the simultaneously hydrodynamically developing flow as well as the thermally developing flow in the rectangular microchannels, their limited analytical results covered only straight ducts with aspect ratio larger than 1. Furthermore, the conventional equivalent method to analyze the flow and the heat transfer involved only the parameters of the inlet and the outlet, which cannot effectively reflect the variations along the channel branching length in the fractal-like microchannels. In order to solve the above problems, a numerical model of a fractal-like microchannel network was formulated to solve the conjugate flow and heat transfer under the simultaneously hydrodynamically and thermally developing flow condition. The subsectional linear integral method taking the flow bifurcations into account was adopted to compare with the conventional equivalent method, and the results were verified by the experiments conducted on two different boundary conditions. Our studies will be presented in two parts: (1) the present paper is Part A which focused on the comparisons of numerical analysis methods to determine the friction factor and the Nusselt number and (2) the performance coefficients of the heat transfer and the pressure drop for fractal-like microchannel networks will be presented in Part B [39].

2. Numerical analyses of the fractal-like microchannel networks

2.1. Hydrodynamic analysis: full developed flow and developing flow

Since the pressure drop along the axial length is much larger than that in the radial direction, it is appropriate to use one-dimensional method to calculate the main pressure loss. For Newtonian incompressible fluid in a smooth channel, the pressure drop comes mainly from the frictional force due to the shear stress at the wall. So the frictional pressure drop ΔP over a length L is obtained:

$$\Delta P = \frac{2f\rho u_m^2 L}{D_h} \tag{1}$$

where ρ is the density of the fluid, u_m is the average flow velocity of the fluid, D_h is the hydraulic diameter of the channel, f is the Fanning frictional factor used in the microchannel depending on the flow conditions, the channel wall geometries, and the surface conditions. For the fully developed laminar flow in a rectangular channel, Shah and London [40] provided the following empirical equation for friction factor:

$$Po = f\mathrm{Re} = 24(1 - 1.3553\alpha + 1.9467\alpha^2 - 1.7012\alpha^3 + 0.9564\alpha^4 - 0.2537\alpha^5) \tag{2}$$

where Po is the Poiseuille number, Re is the Reynolds number, and α is the aspect ratio, defined as the ratio of the channel height to its width. It is noted to see that only the aspect ratio is a crucial factor to decide the friction factor in the fully developed flow. For the fractal-like microchannel network studied, the largest roughness was measured by a SEM to be 0.07 μm, 0.056% of the shortest dimension of the channel. So the inner wall was treated as a smooth surface with negligible fluid slip [28,41]. Since the highest Reynolds number for this study was below 2000, as a result, the flow regime was treated as laminar. Thus the pressure drop depends primarily on the channel geometrical configuration and the flow developing situations along the channel length. According to the boundary layer theory, when the fluid enters a channel with uniform velocity, the velocity profile begins to develop along its length until reaching the fully developed Hagen–Poiseuille velocity. Then the hydrodynamically developing region L_h is defined by the following equation [42]:

$$\frac{L_h}{D_h} = 0.05\mathrm{Re} \tag{3}$$

Since the dimensions of fractal-like microchannel networks in many applications are small, the flow length in the developing region therefore forms a major portion of the whole channel length with high pressure gradient. Thus the pressure drop in this kind of channel over a length x from the entrance is expressed as [42]:

$$\Delta P = \frac{2f_{app}\rho u_m^2 x}{D_h} = \frac{2(f\mathrm{Re})\mu u_m x}{D_h^2} + K(x)\frac{\rho u_m^2}{2} \tag{4}$$

where μ is the dynamic viscosity and f_{app} is the apparent friction factor, accounting for the pressure drop due to the friction and the developing region effects. It is noted that f_{app} represents an average value of the friction factor over the flow length between the entrance section and the location under consideration. $K(x)$ is an incremental pressure defect between the apparent friction factor f_{app} and the fully developed Fanning friction factor f over a length x, i.e., $K(x) = (f_{app} - f)4x/D_h$. For $x > L_h$, where the flow is mainly in the fully developed region, the incremental pressure defect attains a constant value $K(\infty)$, known as the Hagenbach's factor which depends only on the Reynolds number. For $x < L_h$, Phillips [43] gave the tabulated values of the apparent friction factor versus channel aspect ratio for the range of non-dimensionalized lengths $x^+ = (x/D_h)/\mathrm{Re}$ from 0 to 1.

2.2. Thermal analysis: developing flow and fully developed flow

The Nusselt number in the fully developed laminar flow is constant, depending on the channel geometry and the wall heat transfer boundary condition. For a rectangular channel with a constant wall temperature (T-boundary condition), the Nusselt number is given below [42]:

$$Nu_T = 7.541\left(1 - 2.610\alpha + 4.970\alpha^2 - 5.119\alpha^3 + 2.702\alpha^4 - 0.548\alpha^5\right) \tag{5}$$

However, in the developing region, the Nusselt number will increase with the Reynolds number, depending on the channel aspect ratio α and the wall boundary conditions. The thermal entry length L_t in a rectangular channel is expressed as [42]:

$$\frac{L_t}{D_h} = 0.1\,Re\,Pr \tag{6}$$

where Pr is the Prandtl number. The heating in microchannel geometries for the present study comes from two side walls and the bottom wall since an adiabatic cover of epoxy glass bonded on the top of the microchannels to form the flow passage. The Nusselt number in the thermally developing flow region is derived from Phillips [44]:

$$Nu_{x,3}(x^*, \alpha) = Nu_{x,4}(x^*, \alpha)\frac{Nu_{fd,3}\left(x^* = x_{fd}^*, \alpha\right)}{Nu_{fd,4}\left(x^* = x_{fd}^*, \alpha\right)} \tag{7}$$

where $x^* = (x/D_h)/Re\,Pr$ is the non-dimensionalized length for thermal analysis and α_c lies within $0.1 < \alpha_c < 10$. The subscripts x, 3 and x, 4, respectively, refer to the location at a distance x in the heated length for the three-sided and the four-sided heating cases. The subscript fd indicates that the flow is fully developed. The Nusselt numbers in the fully developed region for both heating conditions and in the developing region for the four-sided heating condition were presented by Kandlikar et al. [42].

2.3. Subsectional integral method

For a straight microchannel, it is appropriate to use the above equations directly along the channel length to calculate the friction factor according to the pressure drop between the inlet and outlet of the channel. And the Nusselt number can be expressed in terms of the Reynolds number and the channel aspect ratio [42]. But for a fractal-like microchannel network, the friction factor together with the Nusselt number is nonlinear, fluctuating with the branching channel length in the developing flow region, as shown in Fig. 1, based on the above analysis. Due to the secondary flow and recirculation flow motions initiated at the bifurcations and bends, the developing flow regenerates again and maintain along the subsequent straight channel until reaching the next bifurcation or bend, which keeps the flow always in the developing region. Under such a situation, the conventional equivalent numerical analysis only accounts for the inlet and outlet parameters and the aspect ratio of concern which would bring about deviations in determining the flow and heat transfer characteristics. Therefore, the subsectional integral calculation method has been put forward to take the bifurcation effects into consideration.

The friction factor and Nusselt number will be integrated along each branching length and then averaged by the total length of the channel:

$$\bar{f} = \frac{1}{x^+}\int_0^{x^+} f_x dx^+ = \frac{1}{x^+}\left[\int_0^{x_1^+} f_1 dx^+ + \int_{x_1^+}^{x_2^+} f_2 dx^+ + \cdots + \int_{x_{n-1}^+}^{x_n^+} f_x dx^+\right] \tag{8}$$

$$\overline{Nu} = \frac{1}{x^*}\int_0^{x^*} Nu_x dx^* = \frac{1}{x^*}\left[\int_0^{x_1^*} Nu_1 dx^* + \int_{x_1^*}^{x_2^*} Nu_2 dx^* + \cdots + \int_{x_{n-1}^*}^{x_n^*} Nu_x dx^*\right] \tag{9}$$

where x^+ and x^* represent the characteristic lengths of the friction factor and the Nusselt number, the subscript n represents the number of the level, f_x and Nu_x are the local friction factor and the local Nusselt number of each branch in the developing region.
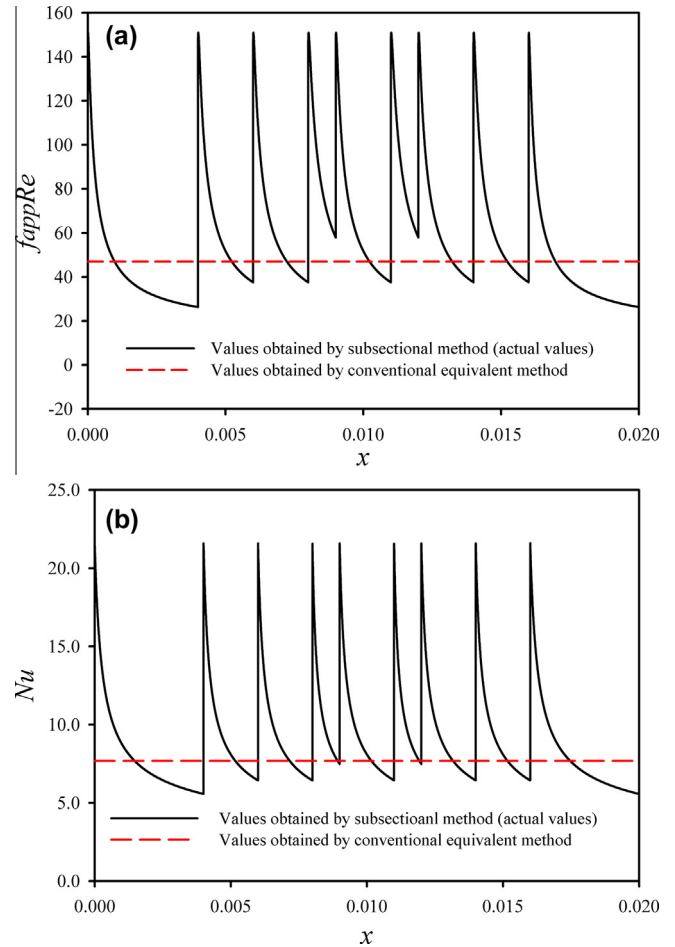
Fig. 1. Changing trend of the friction factor and the Nusselt number along the channel length with two branching levels in the fractal-like microchannel network: (a) friction factor (b) Nusselt number.

3. Experimental measurement system

The schematics of the fractal-like microchannel networks used in the current study are shown in Fig. 2, with one and two branching levels. The height of the entire channels for all the networks was 125 μm, while the maximum percentage uncertainty encountered
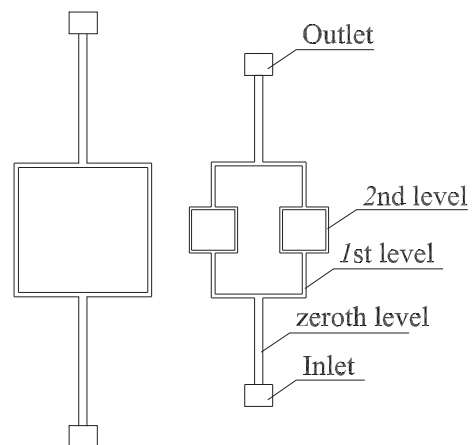
Fig. 2. Schematics of the fractal-like microchannel networks: (a) one branching level (b) two branching levels.

was 5%. The widths were 125 μm, 250 μm, and 375 μm corresponding to the aspect ratios of 1, 0.5 and 0.333, respectively, for three kinds of fractal-like microchannel networks. The channel length was 4000 μm at the zeroth level, 2000 μm at the 1st level and 1000 μm at the 2nd level. The classifications of the test cases are given in Table 1. For the purpose of comparison among the fractal-like microchannel configurations with different aspect ratios and branching levels, all the analyses was conducted under the same convective heat transfer area.

The experimental apparatus used in the present study was composed of three parts: the test section, the water driving system, and the dynamic data acquisition system, as shown in Fig. 3. In addition, deionized water (DI water) was used as the working fluid with the thermophysical properties shown in Table 2. The systematic measurements included: (1) the pressure drop between the inlet and outlet through a fractal-like microchannel network; (2) the water temperatures at the inlet and outlet; (3) the wall heated temperatures on the bottom of the fractal-like microchannel network; (4) the ambient temperature and the water temperature in the reservoir; (5) the mass flow rate of water flowing through the fractal-like microchannel network.

The test section, as shown in the magnified part of Fig. 3, was composed of a Pyrex glass cover block, a fractal-like microchannel silicon test chip, a brass heat spreading plate, a thermoelectric cooling chip (as the heat source, which was controlled by a DC voltage source to provide low electric voltage and high current), a thermal insulation layer, and a polymethylmethacrylate (PMMA) base plate with the inlet and outlet manifolds. Four calibrated T-type (Cu/Cu–Ni, accuracy:±0.1 K) thermocouples along the stream-wise direction (temperature readings T_1, T_2, T_3, and T_4, as shown in Fig. 3) were embedded into four small cavities on the top surface of the brass plate. A thin silicon thermal grease layer was coated between the contact surfaces of the test chip and the brass plate to ensure a close contact of the surfaces, resulting in a negligible thermal resistance between the brass plate and the silicon test chip. Thus the mean temperature of the four thermocouples' readings ($T_m = (T_1 + T_2 + T_3 + T_4)/4$) was used to be the constant channel wall temperature of the test chip.

To drive the DI water flow into the microchannels, a precision-controlled high performance liquid chromatography pump (HPLC, made by Jasco, Model PU-2087+, operating range: 0–80 KPa, accuracy: ±0.02%) was used to provide the desired constant flow rates ranging from 0.5 ml/min to 30 ml/min. A diaphragm type differential pressure transducer (made by Druck, Model PMP4110, operating range: 0–7 bar, accuracy: ±0.05%) was connected to the sumps of PMMA to measure the corresponding pressure drop across the inlet and outlet of the microchannel network. Extreme caution was exercised to ensure that no visible dead volume was presented. A digital electronic balance (made by Sartorius, Model TE214S, accuracy: 0.001 g) was used to measure the weight of the accumulated mass of the DI water in a specified time interval to obtain the mass flow rate of the system.

Two calibrated K-type (Ni–Cr/Ni–Si, accuracy: ±0.1 K) thermocouples were placed at the inlet and outlet of the test section with temperature reading T_i and T_o, respectively, to measure the temperatures of the DI water at the entrance and the exit of the channel. Meanwhile, the temperature of the water in the reservoir was monitored by a T-type thermocouple to ensure that the inlet temperature of the DI water was maintained at a constant value of 297 K by a space temperature control device.

For each measurement, the pressure and temperature readings were collected automatically by a data acquisition system (made by Yokogawa, Model MX1000). Before measurements began, the channels and connecting tubes were filled with DI water under pressure to ensure that there were no bubbles inside the system under test. Then the system was kept running for a time period from 30 min to 2 h until the four thermocouples' readings of the channel wall were stable and maintained at a constant temperature of 323 K.

4. Results and discussions

For the fractal-like microchannel network used in this study, according to Eqs. (3) and (5), with the aspect ratio $\alpha = 1$, at the main channel (the branching level number $n = 0$), the length of the hydrodynamically developing region L_h was determined to be 87.9% of the channel length. For other channels with all the aspect ratios and branching level numbers, both the lengths of the hydrodynamically and thermally developing region, L_h and L_t, were longer than the lengths of all branching channels. As a result, the analyses conducted in the study needed to account for these two kinds of developing flow effects, and then the friction factor was expressed by the apparent friction factor unless this term was specified differently. The numerical simulations were carried out by the software package CFD-ACE+2006, based on the finite volume method (FVM). Subsequently, the results obtained by the

Table 1
Classifications of fractal-like microchannel networks.

Aspect ratio α	One branching level	Two branching levels
1	125-1	125-2
0.5	250-1	250-2
0.333	375-1	375-2

Table 2
Thermophysical properties of DI water and silicon within the temperature range of 283–373 K.

Signal	Unit	DI water	Silicon
μ	Pa·s	$0.0194 - 1.065e\text{-}04 \times T + 1.489e\text{-}07 \times T^2$	
λ	W/(m·K)	$-0.829 + 0.0079 \times T - 1.04e\text{-}05 \times T^2$	$290 - 0.4 \times T$
c_p	J/(kg·K)	$5348 - 7.42 \times T + 1.17e\text{-}02 \times T^2$	$390 + 0.9 \times T$
ρ	kg/m³	998.2	2330
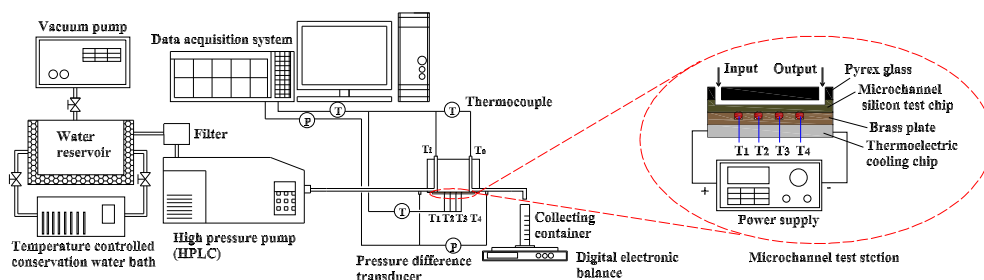
Fig. 3. Schematic diagram of the experimental apparatus for the fractal-like microchannel network.

experiments were compared with those obtained by the numerical analyses using the conventional equivalent method and the subsectioanl integral method, respectively, with the cases of the same boundary conditions and initial parameters. Moreover, two different boundary conditions were used to determine the deviations resulting from the numerical calculations and experimental data. The results discussed in Section 4.1 below were for the case with a constant temperature difference between the inlet and the outlet, while those in Section 4.2 were for the case with a constant volumetric flow rate.

4.1. Comparisons of friction factors and Nusselt numbers between two methods

For the friction factors, comparisons of the average deviations obtained from the calculated results (by the two evaluation methods – the conventional equivalent method and the subsectioanl integral method) with the experimental results are shown in Table 3. It is clear to see that the accuracy of the calculated results by using the subsectional integral method is much better than those by using the conventional equivalent method. The deviation decreases with a decrease in branching level number since the pressure loss increases with an increase in the branching level number. Fig. 4 shows the results of the friction factor versus the Reynolds number obtained from two numerical methods and the experiments for the fractal-like microchannel network with different aspect ratios and branching levels. The friction factors obtained from the conventional equivalent method are lower than those

Table 3
Average deviations of friction factors obtained from two numerical methods.

Type of microchannels	Conventional equivalent method	Subsectional integral method
125-1	46.3%	5.2%
125-2	63.2%	22.8%
250-1	32.6%	9.2%
250-2	70.3%	23.5%
375-1	45.2%	10.5%
375-2	68.9%	20.2%

obtained from the subsectional integral method. With an increase in the Reynolds number, the deviations between the results obtained from the experiments and those obtained from the conventional equivalent method increase since the high Reynolds number results in the high pressure loss. In summary, the total average deviation relative to the experimental results for the conventional equivalent method in determining the friction factor is 49.93%, while it is 13.94% for the subsectional integral method. As a conclusion, it is recommended that the subsectional integral method rather than the conventional equivalent method be used for the fractal-like microchannel network.

Compared with the experimental data, the average deviations of the Nusselt numbers obtained by the conventional equivalent method and the subsectional integral method are shown in Table 4. It is found that the average deviations resulting from the conventional equivalent method are close to one another (on the order of about 40% deviation). Results of the Nusselt numbers versus
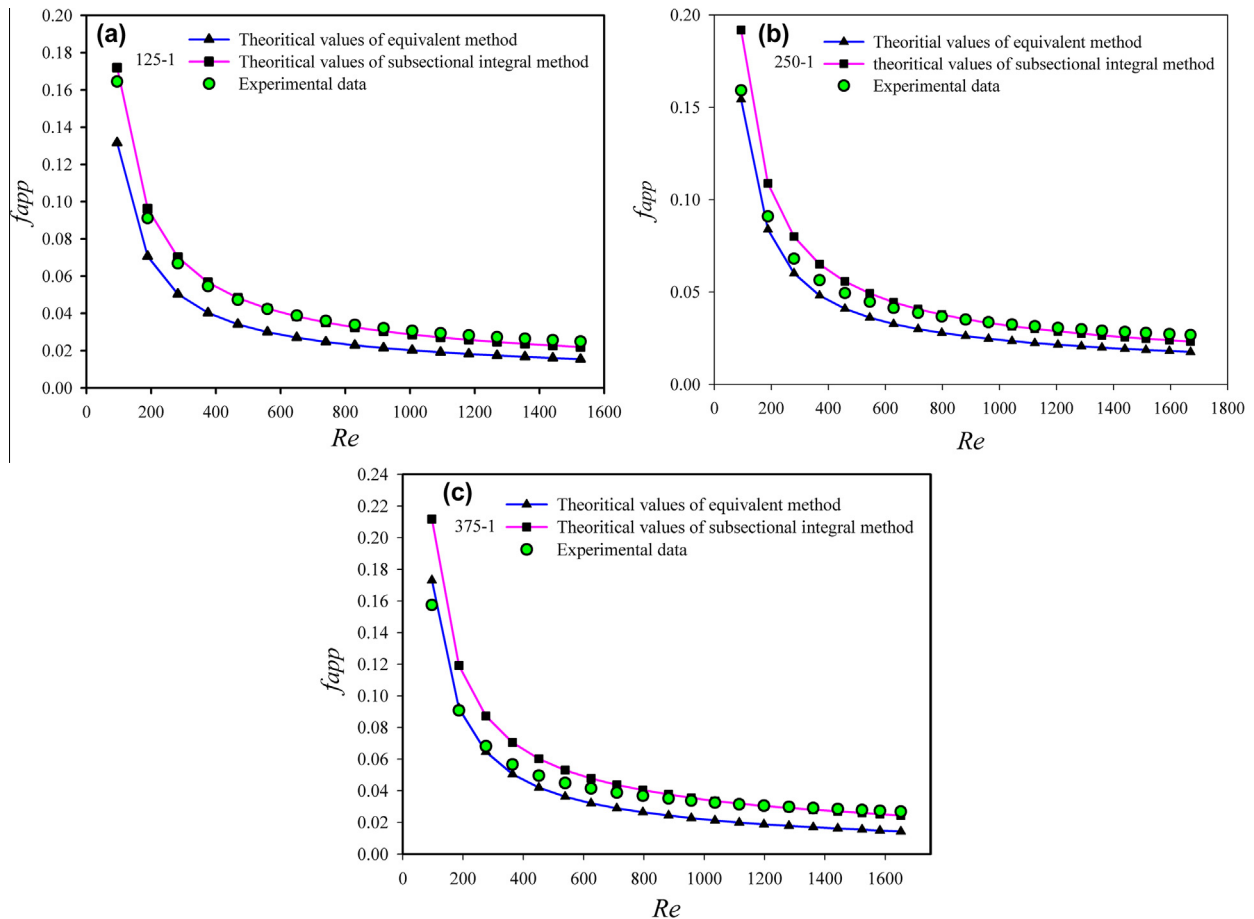
Fig. 4. Friction factors obtained by the conventional equivalent method, the subsectional integral method, and experiments for the fractal-like microchannel networks with one branching levels.

Table 4
Average deviations of the Nusselt numbers obtained from two numerical methods.

Type of microchannels	Conventional equivalent method	Subsectional integral method
125-1	40.9%	7.8%
125-2	43.6%	7.3%
250-1	35.7%	14.0%
250-2	40.0%	10.3%
375-1	39.6%	20.3%
375-2	42.4%	14.9%

the Reynolds numbers of the fractal-like microchannel networks with different aspect ratios and branching levels are shown in Fig. 5. The values of deviation obtained by the conventional equivalent method in all cases increase with the Reynolds number. For the subsectional integral method, the average deviations of the Nusselt number increase with a decrease in the aspect ratio and the branching level. Moreover, when the Reynolds number is higher than 800, the deviation of the subsectional integral method has a decline trend and the calculation results even coincide with the experimental results in the range of Re > 1100. This kind of phenomenon may attribute to the design of the experimental apparatus. Before entering the microchannels, there is a small tank for storing water. As a consequence, when the flow rate is very low, the water is heated in advance before entering the channel. Thus the temperature difference of the water decreases due to the heat loss. As a result, the Nusselt numbers obtained from the experimental data in the high Reynolds number region are in agreement

with those obtained from the numerical analyses. However, from the overall trend, it is concluded that the heat transfer results obtained by using the subsectional integral method are in better agreement with the experimental results compared with those obtained by using the conventional equivalent method.

4.2. Comparisons of friction factors and Nusselt numbers between the numerical calculations and the experimental data

In order to further validate the flow and heat transfer obtained by using the subsectional integral method, experiments were carried out under the constant volume flow rate. And parameters of the numerical analysis were kept to be the same as those used in the experiments. Figs. 6 and 7 are the curves obtained from the experiments for the friction factors and the Nusselt numbers together with those obtained from the numerical analyses. Fig. 6(a) and (b) show that the friction factors with two branching levels are somewhat higher than those with one branching level. Besides, for the same branching level, the smaller the aspect ratio α is, the bigger the friction factor due to the effect of the larger hydraulic diameter and viscous force. Similarly, the fractal-like microchannel network with two branching levels has higher Nusselt numbers as shown in Fig. 7. And the Nusselt number increases with a decrease in the aspect ratio. The reason for the deviations between the numerical and the experimental results in the range of low Reynolds numbers has been explained in Section 4.1. In general, the flow and the heat transfer obtained from the numerical analyses using the subsectional integral method are in good agreement with
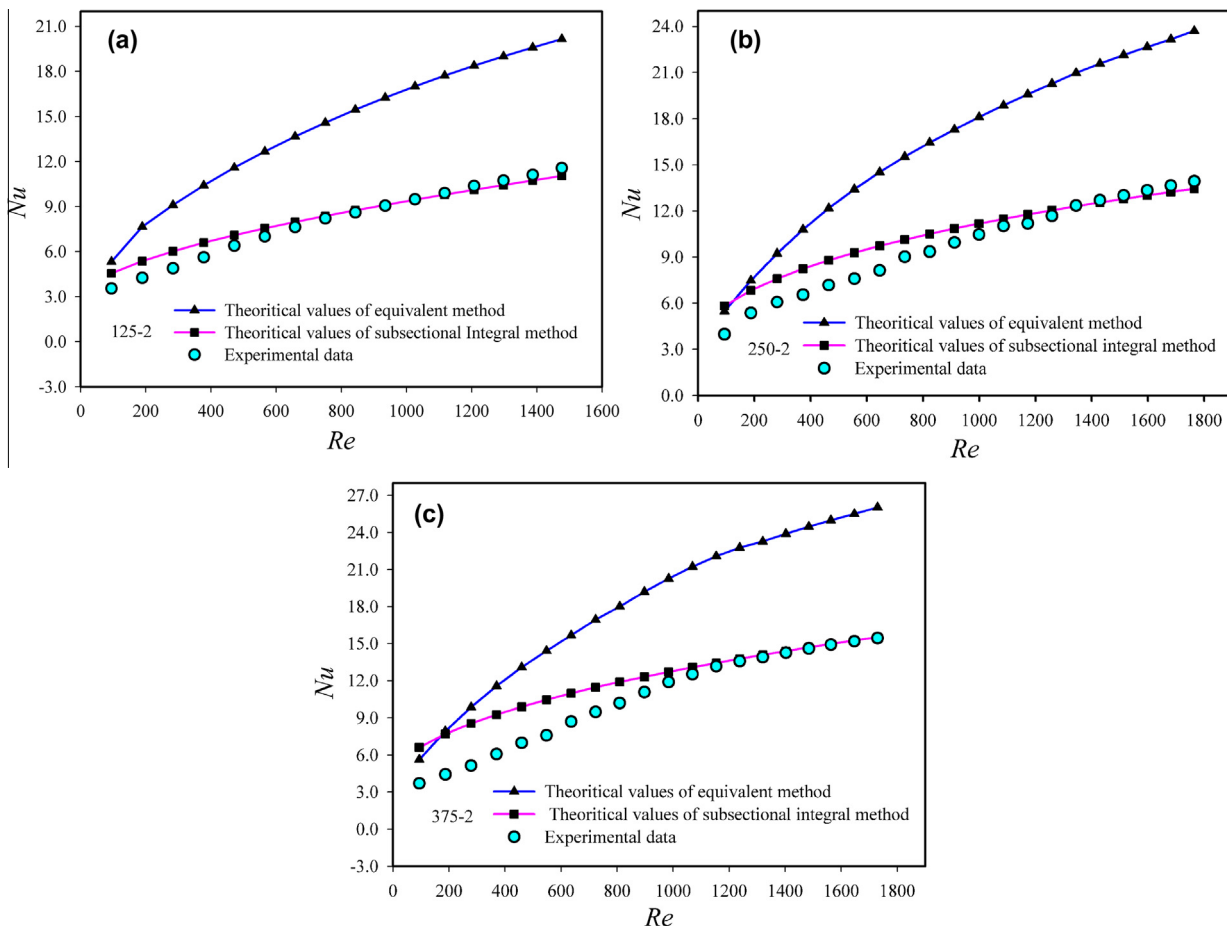
Fig. 5. Nusselt numbers obtained by the conventional equivalent method, the subsectional integral method and experiments for the fractal-like microchannel networks with two branching levels.
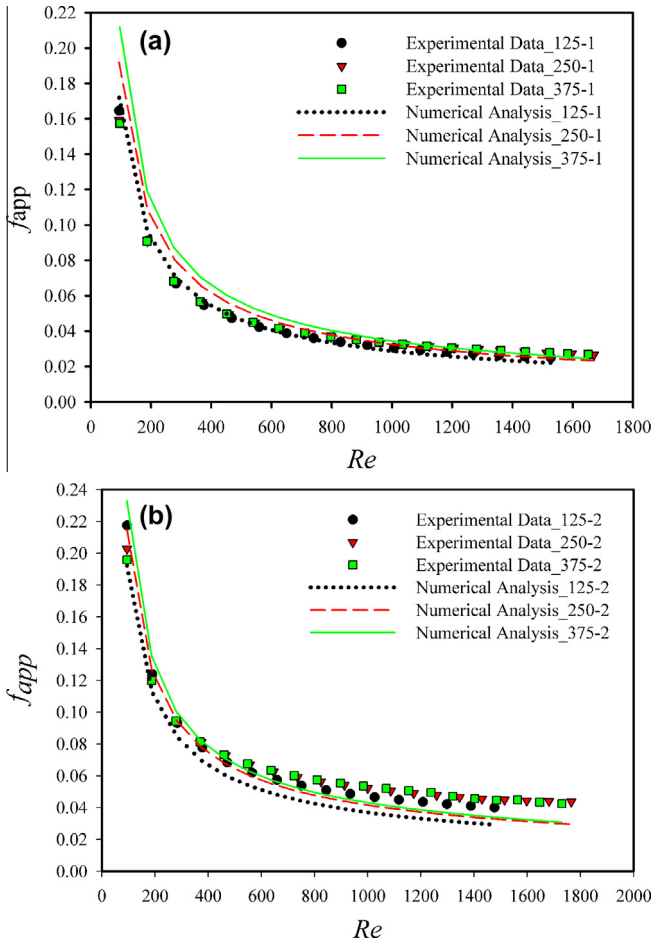
Fig. 6. Friction factors of the numerical and experimental results for fractal-like microchannel networks: (a) one branching level (b) two branching levels.

Fig. 7. Nusselt numbers of the numerical and experimental results for fractal-like microchannel networks: (a) one branching level (b) two branching levels.

those obtained from the experimental data, and the trends of the deviation between them are of the same order of magnitude as those documented in Section 4.1.

5. Conclusions

The friction factors and the Nusselt numbers of the fractal-like microchannel networks were investigated in this study. Two important aspects of the flow behavior under consideration have been developed and discussed: one was the effects of the hydrodynamically and thermally developing flow on the performance of the flow and heat transfer, the other was the development of the numerical analysis of the subsectional integral method to account for these effects. The conclusions obtained from this study were as follows:

(1) For the fractal-like microchannel networks used in the present paper, the fractals made the hydrodynamic and thermal entry lengths to be comparable with or even longer than the lengths of channels; the assumption of the fully developed flow neglecting the effects of the developing flow on the flow and heat transfer was inadequate. Therefore, the apparent friction factor accounting for the pressure drop due to the friction and the developing region effects was employed to replace the Fanning friction factor.

(2) Aiming at the configuration of fractal-like microchannel networks, the flow and heat transfer obtained by using the subsectional integral method in the numerical analysis were

compared with those obtained by using the conventional equivalent method. The deviations of the calculated results of the friction factors and Nusselt numbers were presented by using the two methods. As a conclusion, the conventional equivalent method had larger discrepancies for both friction factors and the Nusselt numbers. And the deviations increased with an increase in the Reynolds number.

(3) The results of the friction factors and the Nusselt numbers obtained by using the newly developed subsectional integral method in the present study were found to be in good agreement with those obtained from the experimental data.

The conclusions provided above would provide useful information for further investigations on the fractal-like microchannel networks or other complex configurations. The subsequent paper (Part B of this study) regarding the determination of the performance of fractal-like microchannel networks is to be presented, based on the above research work.

References

[1] D.B. Tuckerman, R.F.W. Pease, High-performance heat sinking for VLSI, IEEE Electron. Electron. Device Lett. 2 (1981) 126–127.

[2] W. Urbanek, J.N. Zemel, Investigation of the temperature dependence of Poiseuille numbers in microchannel flow, J. Micromech. Microeng. 3 (1993) 206–209.

[3] X.F. Peng, G.P. Peterson, Convective heat transfer and flow friction for water flow in microchannel structures, Int. J. Heat Mass Transfer 39 (1996) 2599–2608.

[4] S.M. Flockhart, R.S. Dhariwal, Experimental and numerical investigation into the flow characteristics of channels etched in ⟨100⟩ silicon, Trans. ASME J. Fluids Eng. 120 (1998) 291–295.

[5] P.S. Lee, S.V. Garimella, D. Liu, Investigation of heat transfer in rectangular microchannels, Int. J. Heat Mass Transfer 48 (2005) 1688–1704.

[6] X.Q. Wang, C. Yap, A.S. Mujumdar, Effects of two-dimensional roughness in flow in microchannels, J. Electron. Packag. 127 (2005) 357–361.

[7] K.C. Toh, X.Y. Chen, J.C. Chai, Numerical computation of fluid flow and heat transfer in microchannels, Int. J. Heat Mass Transfer 45 (2005) 5133–5141.

[8] J. Li, G.P. Peterson, 3-Dimensional numerical optimization of silicon-based high performance parallel microchannel heat sink with liquid flow, Int. J. Heat Mass Transfer 50 (2007) 2895–2904.

[9] P.S. Lee, S.V. Garimella, D. Liu, Saturated flow boiling heat transfer and pressure drop in silicon microchannel arrays, Int. J. Heat Mass Transfer 51 (2008) 789–796.

[10] J.D. Mlcak, N.K. Anand, M.J. Rightley, Three-dimensional laminar flow and heat transfer in a parallel array of microchannels etched on a substrate, Int. J. Heat Mass Transfer 51 (2008) 5182–5191.

[11] W. Escher, B. Michel, D. Poulikakos, Efficiency of optimized bifurcating tree-like and parallel microchannel networks in the cooling of electronics, Int. J. Heat Mass Transfer 52 (2009) 1421–1430.

[12] A. Bejan, Constructal-theory network of conducting paths for cooling a heat generating volume, Int. J. Heat Mass Transfer 40 (1997) 799–815.

[13] A. Bejan, M.R. Errera, Deterministic tree networks for fluid flow: geometry for minimal flow resistance between a volume and one point, fractals-an interdisciplinary, J. Complax Geom. Nat. 5 (1997) 685–695.

[14] A. Bejan, The tree of convective heat streams: its thermal insulation function and the predicted 3/4 power relation between body heat loss and body size, Int. J. Heat Mass Transfer 44 (2001) 699–704.

[15] A. Bejan, Design with Constructal Theory, Wiley, Hoboken, 2008.

[16] D.V. Pence, Reduced pumping power and wall temperature in microchannel heat sinks with fractal-like branching channel networks, Microscale Therm. Eng. 6 (2002) 319–330.

[17] A.Y. Alharbi, D.V. Pence, N.R. Cullion, Fluid flow through microscale fractal-like branching channel networks, J. Fluids Eng. 6 (2003) 1051–1057.

[18] A.Y. Alharbi, D.V. Pence, N.R. Cullion, Thermal characteristics of microscale fractal-like branching channels, J. Heat Transfer 126 (2004) 744–782.

[19] D. Heymann, D.V. Pence, V. Narayanan, Optimization of fractal-like branching microchannel heat sinks for single-phase flows, Int. J. Therm. Sci. 49 (2010) 1383–1393.

[20] B.J. Daniels, J.A. Liburdy, D.V. Pence, Adiabatic flow boiling in fractal-like microchannels, Heat Transfer Eng. 28 (2007) 817–825.

[21] B.J. Daniels, J.A. Liburdy, D.V. Pence, Experimental studies of adiabatic flow boiling in fractal-like branching microchannels, Exp. Therm. Fluid Sci. 35 (2011) 1–10.

[22] S.M. Senn, D. Poulikakos, Tree network channels as fluid distributors constructing double-staircase polymer electrolyte fuel cells, J. Appl. Phys. 96 (2004) 842–852.

[23] S.M. Senn, D. Poulikakos, Laminar mixing, heat transfer and pressure drop in tree-like microchannel nets and their application for thermal management in polymer electrolyte fuel cells, J. Power Sources 130 (2004) 178–191.

[24] S.M. Senn, D. Poulikakos, Pyramidal direct methanol fuel cells, Int. J. Heat Mass Transfer 49 (2006) 1516–1528.

[25] X.Q. Wang, A.S. Mujumdar, C. Yap, Numerical analysis of blockage and optimization of heat transfer performance of fractal-like microchannel nets, J. Electron. Packag. 128 (2006) 38–45.

[26] X.Q. Wang, A.S. Mujumdar, C. Yap, Thermal characteristics of tree-shaped microchannel nets for cooling of a rectangular heat sink, Int. J. Therm. Sci. 45 (2006) 1103–1112.

[27] X.Q. Wang, A.S. Mujumdar, C. Yap, Effect of bifurcation angle in tree-shaped microchannel networks, J. Appl. Phys. 102 (2007) 1–8. 073530.

[28] X.Q. Wang, C. Yap, A.S. Mujumdar, Effects of two-dimensional roughness in flow in microchannels, J. Electron. Packag. 27 (2005) 357–361.

[29] Y.P. Chen, P. Cheng, Heat transfer and pressure drop in fractal tree-like microchannel nets, Int. J. Heat Mass Transfer 45 (2002) 2643–2648.

[30] Y.P. Chen, P. Cheng, An experimental investigation on the thermal efficiency of fractal tree-like microchannel nets, Int. J. Heat Mass Transfer 32 (2005) 931–938.

[31] Y.P. Chen, C.B. Zhang, M.S. Shi, Y.C. Yang, Thermal and hydrodynamic characteristics of constructal tree-shaped minichannel heat sink, AIChE J. 56 (2010) 2018–2029.

[32] Y. Chen, C.B. Zhang, M.S. Shi, Methanol steam reforming in microreactor with constructal tree-shaped network, J. Power Sources 196 (2011) 6366–6373.

[33] C. Zhang, Y. Chen, Flow boiling in constructal tree-shaped minichannel network, Int. J. Heat Mass Transfer 54 (2011) 202–209.

[34] D. Haller, P. Woias, N. Kockmann, Simulation and experimental investigation of pressure loss and heat transfer in microchannel networks containing bends and T-junctions, Int. J. Heat Mass Transfer 52 (2009) 2678–2689.

[35] U. Soupremanien, S.L. Person, M.F. Marinet, Y. Bultel, Influence of the aspect ratio on boiling flows in rectangular mini-channels, Exp. Therm. Fluid Sci. 35 (2011) 797–809.

[36] T.M. Adams, M.J. Kazmierczak, F.M. Gerner, Developing convective heat transfer in deep rectangular microchannels, Int. J. Heat Fluid Flow 20 (1999) 149–157.

[37] P.S. Lee, S.V. Garimella, D. Liu, Investigation of heat transfer in rectangular microchannels, Int. J. Heat Mass Transfer 48 (2005) 1688–1694.

[38] P.S. Lee, S.V. Garimella, D. Liu, Thermally developing flow and heat transfer in rectangular microchannels of different aspect ratios, Int. J. Heat Mass Transfer 49 (2006) 3060–3067.

[39] C.P. Zhang, Y.F. Lian, X.F. Yu, W. Liu, J.T. Teng, T.T. Xu, C.H. Hsu, Y.J. Chang, R. Greif, Numerical and experimental studies on laminar hydrodynamic and thermal characteristic in fractal-like microchannel networks. Part B: Investigations on the performances of pressure drop and heat transfer, Int. J. Heat Mass Transfer, in press.

[40] R.K. Shah, A.L. London, Laminar Flow Forced Convection in Ducts, Supplement 1 to Advances in Heat Transfer, Academic Press, New York, 1978.

[41] N.V. Priezjev, S.M. Troian, Influence of periodic wall roughness on the slip behavior at liquid/solid interfaces: molecular versus continuum predictions, J. Fluid Mech. 554 (2006) 25–46.

[42] S.G. Kandlikar, S. Garimella, D.Q. Li, S. Colin, M.R. King, Heat Transfer and Fluid Flow in Minichannels and Microchannels, Elsevier limited, Oxford, 2006.

[43] R.J. Phillips, Forced convection, liquid cooled, microchannel heat sinks, MS Thesis, Massachusetts Institute of Technology, Cambridge, MA, 1987.

[44] R.J. Phillips, Microchannel heat sinks, in: Advances in Thermal Modeling of Electronic Components and Systems, Hemisphere Publishing Corporation, New York, 1990.